

## Extremely large and hot multilayer Keplerian disk around the O-type protostar W51N: The precursors of the HCHII regions?

Luis A. Zapata<sup>1</sup>

*Centro de Radioastronomía y Astrofísica, UNAM, Apdo. Postal 3-72 (Xangari), 58089 Morelia, Michoacán, México*

Ya-Wen Tang

*Academia Sinica Institute of Astronomy and Astrophysics, Taipei, Taiwan*

Silvia Leurini

*Max-Planck-Institut für Radioastronomie, Auf dem Hügel 69, 53121, Bonn, Germany*

### ABSTRACT

We present sensitive high angular resolution ( $0.57''$ - $0.78''$ ) SO, SO<sub>2</sub>, CO, C<sub>2</sub>H<sub>5</sub>OH, HC<sub>3</sub>N, and HCOCH<sub>2</sub>OH line observations at millimeter and submillimeter wavelengths of the young O-type protostar W51 North made with the Submillimeter Array (SMA). We report the presence of a large (of about 8000 AU) and hot molecular circumstellar disk around this object, which connects the inner dusty disk with the molecular ring or toroid reported recently, and confirms the existence of a single bipolar outflow emanating from this object. The molecular emission from the large disk is observed in layers with the transitions characterized by high excitation temperatures in their lower energy states (up to 1512 K) being concentrated closer to the central massive protostar. The molecular emission from those transitions with low or moderate excitation temperatures are found in the outermost parts of the disk and exhibits an inner cavity with an angular size of around  $0.7''$ . We modeled all lines with a Local Thermodynamic Equilibrium (LTE) synthetic spectra. A detail study of the kinematics of the molecular gas together with a LTE model of a circumstellar disk shows that the innermost parts of the disk are also Keplerian plus a contracting velocity. The emission of the HCOCH<sub>2</sub>OH reveals the possible presence of a warm “companion” located to the northeast of the disk, however its nature is unclear. The emission of the SO and SO<sub>2</sub> is observed in the circumstellar disk as well as in the outflow. We suggest that the massive protostar W51 North appears to be in a phase before the presence of a Hypercompact or an Ultracompact HII (HC/UCHII) region, and propose a possible sequence on the formation of the massive stars.

---

<sup>1</sup>Max-Planck-Institut für Radioastronomie, Auf dem Hügel 69, 53121, Bonn, Germany

*Subject headings:* stars: pre-main sequence – ISM: jets and outflows – ISM: individual: (W51 North) – techniques: spectroscopic ISM: molecules

## 1. Introduction

It is thought that the Hypercompact or Ultracompact HII (HCHII or UCHII) regions trace early stages of massive star formation after the hot molecular core phase. However, the physical processes involved in this transition are still poorly understood (see for reviews: Kurtz 2005; Lizano 2008). The appearance of one HCHII begins when the Lyman continuum output from a massive young star becomes sufficient high to ionize its surroundings. These objects show a rising continuum spectra,  $S_\nu \propto \nu^\alpha$ , with a slope  $\alpha \sim 1$ , intermediate between the optically thick and thin limits, small sizes ( $\sim 0.01$  pc), high temperatures ( $10^4$  K), high densities ( $\geq 10^6$  cm $^{-3}$ ), and very broad radio recombination lines ( $\Delta\nu_{FWHM} \geq 40$  km s $^{-1}$ ) indicating both pressure broadening and the presence of bulk motions of dense gas (e.g. Sewilo et al. 2004). On the other hand, the hot molecular cores internally heated by massive protostars are small ( $\sim 0.05$  pc) and compact regions of dense molecular gas ( $\geq 10^6$  cm $^{-3}$ ) which show very rich millimeter and submillimeter spectra (see Kurtz et al. 2000; van der Tak 2004; Cesaroni 2005, for reviews on this topic). The hot molecular core phase begins at much colder temperatures ( $\sim 100$  K) than the HC/UCHII stage.

There are many cases where the UCHII or even the HCHII regions are observed in association with hot cores, some of them are: G5.89-0.39 (Su et al. 2009); G24 A1 (Beltrán et al. 2006); G10.47, and G31.41+0.31 (Cesaroni et al. 2010; Rolffs et al. 2009); W51e2, W51e8, NGC 7538 IRS1, G28.2 and G10.6 (Klaassen et al. 2009); IRAS 17233-3606 (Laurini et al. 2008). However, there are some others cases where the hot cores do not show the presence of a strong HCHII (e.g. AFGL490, NGC 7538S, and IRAS 20126; Nakamura et al. 1991; Schreyer et al. 2002; Cesaroni et al. 2005; Sandell & Wright 2010) possibly because the infalling molecular gas partially quenches its formation (e.g. Walmsley 1995; Osorio et al. 1999) or maybe because the massive central protostar(s) are/is in an early phase with not high enough temperatures to ionize their/its surroundings.

W51 North is one of the youngest massive stars within the luminous cluster W51-IRS2 that is still on the process of formation. This object is associated with a strong mm and submm source, a hot molecular core at an excitation temperature of  $\sim 200$  K (Zhang et al. 1998), no centimeter free-free emission at all ( $\leq 5$  mJy at 1.3 cm) that could be related with an HC/UCHII or a thermal jet (Gaume et al. 1993; Zhang et al. 1998; Eisner et al. 2002). From this object emanates a powerful molecular outflow observed at very small scales by masers spots of SiO and H $_2$ O, and at large scales in thermal SiO( $J = 5 - 4$ ) (Schneps et al. 1981; Eisner et al. 2002; Imai et al. 2002; Zapata et al. 2009). Recently, Zapata et al. (2009) using high angular 1.3 and 0.7 mm continuum, and SO $_2$  line observations made with the Submillimeter Array (SMA) and the Very Large Array (VLA) resolved the large dusty and molecular hot core in a rotating Keplerian ring with a size of  $\sim 8000$  AU (at a distance of  $\sim 6$  kpc: Imai et al. 2002; Barbosa et al. 2008; Xu et al. 2009). This structure surrounds a compact central dusty circumstellar disk with a smaller size of approximately 3000 AU, and

where the molecular northwest(redshifted)-southeast(blueshifted) bipolar outflow emerges. However, the relationship between both circumstellar structures was not clear.

In this paper, we present sensitive high angular resolution SMA submillimeter and millimeter line observations of the W51 North region that were made in an attempt to understand the nature of the circumstellar molecular and dusty structures associated with this young massive protostar. In Section 2 discuss the observations undertook in this study. In Section 3, we present and discuss our SMA millimeter and submillimeter data. Finally, in Section 4, we give the main conclusions of the observations presented here.

Table 1: Observational and physical parameters of the submillimeter and millimeter lines

| Lines   | Rest frequency<br>[GHz] | $E_{lower}$<br>[K] | Range of Velocities<br>[km s <sup>-1</sup> ] | Linewidth<br>[km s <sup>-1</sup> ] | LSR Velocity <sup>a</sup><br>[km s <sup>-1</sup> ] | Peak Flux<br>[Jy Beam <sup>-1</sup> ] |
|---|-------------------------|--------------------|--|------------------------------------|--|---------------------------------------|
| C <sub>2</sub> H <sub>5</sub> OH(37 <sub>8,29</sub> -36 <sub>9,28</sub> ) | 216.8121...             | 715                | +54,+67                                      | 7                                  | 59   | 0.1                                   |
| HCOCH <sub>2</sub> OH(62 <sub>13,49</sub> -62 <sub>12,50</sub> )          | 216.7585...             | 1476               | +54,+66                                      | 8                                  | 59   | 0.4                                   |
| CO( $J = 3 - 2$ ) <sup>b</sup>  | 345.7959...             | 16                 | +20,+120                                     | 50                                 | 60   | 3.0                                   |
| SO(8 <sub>9</sub> -7 <sub>8</sub> ) <sup>c</sup>                          | 346.5284...             | 21                 | +30,+90                                      | 35                                 | 59   | 1.0                                   |
| SO <sub>2</sub> (19 <sub>1,19</sub> -18 <sub>0,18</sub> )                 | 346.6521...             | 151                | +41,+72                                      | 15                                 | 58   | 1.0                                   |
| HC <sub>3</sub> N(38-37) ( $v_l=0$ )                                      | 345.6090...             | 306                | +51,+72                                      | 9                                  | 60   | 2.0                                   |
| HCOCH <sub>2</sub> OH(68 <sub>19,49</sub> -67 <sub>20,48</sub> )          | 337.3988...             | 1512               | +48,+73                                      | 10                                 | 62   | 2.0                                   |

<sup>a</sup>The linewidth and LSR velocity were obtained fitting a Gaussian to the spectra.

<sup>b</sup>Spectra with multiple peaks and in absorption about a LSR velocity of 60 km s<sup>-1</sup>.

<sup>c</sup>Spectra with two peaks.

## 2. Observations

### 2.1. Millimeter

The observations were obtained with the SMA<sup>1</sup> during 2008 January 17. The SMA was in its very extended configuration, which included 28 independent baselines ranging in projected length from 30 to 385 k $\lambda$ . The phase reference center of the observations was R.A. = 19h23m40.05s, decl.= 14°31′05.0″ (J2000.0). The frequency was centered at 217.1049 GHz in the Lower Sideband (LSB), while the Upper Sideband (USB) was centered at 228.1049 GHz. The primary beam of the SMA at 230 GHz has a FWHM of about 60″.

We detected the lines C<sub>2</sub>H<sub>5</sub>OH(37<sub>8,29</sub>-36<sub>9,28</sub>) and HCOCH<sub>2</sub>OH(62<sub>13,49</sub>-62<sub>12,50</sub>) in the LSB. See Table 1 for their rest frequencies and rotational temperatures above of the ground state. The full bandwidth of the SMA correlator was 4 GHz (2 GHz in each band). The SMA digital correlator was configured in 24 spectral windows (“chunks”) of 104 MHz each, with 256 channels distributed over each spectral window,

---

<sup>1</sup>The Submillimeter Array (SMA) is a joint project between the Smithsonian Astrophysical Observatory and the Academia Sinica Institute of Astronomy and Astrophysics, and is funded by the Smithsonian Institution and the Academia Sinica.

providing a resolution of 0.40 MHz (0.56 km s<sup>-1</sup>) per channel. However, in this study we smoothed our spectral resolution to about 1 km s<sup>-1</sup>.

The zenith opacity ( $\tau_{230GHz}$ ), measured with the NRAO tipping radiometer located at the Caltech Submillimeter Observatory, was  $\sim 0.15$ , indicating good weather conditions during the observations. Observations of Uranus provided the absolute scale for the flux density calibration. Phase and amplitude calibrators were the quasars 1925+211 and 2035+109. The uncertainty in the flux scale is estimated to be 15–20%, based on the SMA monitoring of quasars. Observations of Uranus provided the absolute scale for the flux density calibration. Further technical descriptions of the SMA and its calibration schemes can be found in Ho et al. (2004).

The data were calibrated using the IDL superset MIR, originally developed for the Owens Valley Radio Observatory (Scoville et al. 1993) and adapted for the SMA.<sup>2</sup> The calibrated data were imaged and analyzed in the standard manner using the MIRIAD and AIPS packages. We used the ROBUST parameter of the INVERT task of MIRIAD set to 2 to obtain a slightly better sensitivity while losing some angular resolution. The resulting image rms noise of line images was around 30 mJy beam<sup>-1</sup> for each velocity channel (with a smoothed size of 1 km s<sup>-1</sup>) at an angular resolution of 0''57 × 0''42 with a P.A. = 57.6°.

Table 2: Observational parameters of the circumstellar multilayer disk

| Specie  | Central Position          |                            | Flux Density<br>[Jy Beam <sup>-1</sup> km s <sup>-1</sup> ] | Deconvolved Size <sup>a</sup> |           | Approx. cavity size<br>[arcsec <sup>2</sup> ] |
|---|---------------------------|----------------------------|---|-------------------------------|-----------|---|
|   | $\alpha(2000)$<br>[h m s] | $\delta(2000)$<br>[° ' ''] |   | [arcsec <sup>2</sup> ]        | [Degrees] |   |
| SO(8 <sub>9</sub> -7 <sub>8</sub> )                                       | 19 23 40.074              | 14 31 05.70                | 341±20  | 1.78±0.01 × 1.39±0.02         | 171±2     | ~ 0.8   |
| SO <sub>2</sub> (19 <sub>1,19</sub> -18 <sub>0,18</sub> )                 | 19 23 40.071              | 14 31 05.54                | 234±15  | 1.65±0.04 × 1.49±0.03         | 24±6      | ~ 0.7   |
| HC <sub>3</sub> N(38-37) ( $\nu_r=0$ )                                    | 19 23 40.060              | 14 31 05.54                | 88±15   | 1.36±0.04 × 0.93±0.04         | 135±7     | ~ 0.6   |
| C <sub>2</sub> H <sub>5</sub> OH(37 <sub>8,29</sub> -36 <sub>9,28</sub> ) | 19 23 40.041              | 14 31 05.49                | 116±15  | 1.31±0.03 × 0.89±0.03         | 107±7     | ~ 0.8   |
| HCOCH <sub>2</sub> OH(68 <sub>19,49</sub> -67 <sub>20,48</sub> )          | 19 23 40.054              | 14 31 05.44                | 105±13  | 1.14±0.03 × 0.88±0.03         | 99±3      | –   |
| HCOCH <sub>2</sub> OH(62 <sub>13,49</sub> -62 <sub>12,50</sub> )          | 19 23 40.062              | 14 31 05.59                | 9.1±2   | 0.81±0.03 × 0.40±0.09         | 75±3      | –   |
| —Companion  | 19 23 40.077              | 14 31 05.63                | 8.5±1   | 1.27±0.04 × 0.39±0.03         | 74±2      | –   |
| Dusty circumstellar disk <sup>b</sup>                                     |                           |                            |   |                               |           |   |
| 7 mm  | 19 23 40.057              | 14 31 05.67                | –   | 0.58±0.02 × 0.27±0.02         | 70±6      | –   |

<sup>a</sup>The Gaussian fitting was obtained with the task JMFIT of AIPS.

<sup>b</sup>Data obtained from Zapata et al. (2009).

## 2.2. Submillimeter

The observations were obtained with the SMA on 2008 July 13. At the time of these observations the SMA had seven antennas in its extended configuration with baselines ranging in projected length from 30

<sup>2</sup>The MIR-IDL cookbook by C. Qi can be found at <http://cfa-www.harvard.edu/~cqi/mircook.html>

to 255 k $\lambda$ . The primary beam of the SMA at 340 GHz has a FWHM of 37". The molecular emission from the hot core was found well inside of the primary beam.

The receivers were tuned to a frequency of 345.796 GHz in the upper sideband (USB), while the lower sideband (LSB) was centered on 335.796 GHz. The LSB contained line HCOCH<sub>2</sub>OH(68<sub>19,49</sub>-67<sub>20,48</sub>) while the USB the lines SO(8<sub>9</sub>-7<sub>8</sub>), SO<sub>2</sub>(19<sub>1,19</sub>-18<sub>0,18</sub>), CO( $J = 3 - 2$ ), and HC<sub>3</sub>N(38-37) ( $\nu_t=0$ ). See Table 1 for their rest frequencies and lower level energies above the ground energy state. The SMA digital correlator was configured in 24 spectral windows (“chunks”) of 104 MHz each, with 128 channels distributed over each spectral window, thus providing a spectral resolution of 0.81 MHz (0.70 km s<sup>-1</sup>) per channel. However, we smoothed our spectral resolution to 1.0 km s<sup>-1</sup> per spectral channel.

The zenith opacity ( $\tau_{230GHz}$ ) was  $\sim 0.035 - 0.04$ , indicating excellent weather conditions. Observations of titan provided the absolute scale for the flux density calibration. Phase and amplitude calibrators were the quasars 1751+096, and 1925+211. The uncertainty in the flux scale is also estimated to be 15 – 20%, also based on the SMA monitoring of the quasars.

The calibrated data were imaged and analyzed in standard manner using the MIRIAD, and AIPS packages. We also used the ROBUST parameter set to 2. The line image rms noise was around 100 mJy beam<sup>-1</sup> for each velocity channel (with a smoothed size of 1 km s<sup>-1</sup>) at an angular resolution of 0.''78  $\times$  0.''58 with a P.A. = 84.7°.

### 3. Results

In Figure 1, we present the disk/ring/outflow system found towards W51 North using observations of the SiO( $J = 5 - 4$ ), SO<sub>2</sub>(22<sub>2,20</sub>-22<sub>1,21</sub>), and millimeter continuum by Zapata et al. (2009). However, in this image, we have exchanged the SiO emission by the emission of the CO( $J = 3 - 2$ ) presented here for the first time. The CO( $J = 3 - 2$ ) confirms the presence of a single powerful and collimated (15°) bipolar outflow (with the blueshifted side towards the southeast while the redshifted one to the north) emanating from the disk/ring structure at similar scales. However, the CO( $J = 3 - 2$ ) reveals that the outflow extents for a few arcseconds more on both sides in comparison with the emission traced by SiO( $J = 5 - 4$ ), and shows a slightly larger radial velocity range (+30 to +120 km s<sup>-1</sup>). In this image, it is more clear to see the deviation of the blueshifted side of the outflow with respect to the redshifted one than in Zapata et al. (2009).

Figure 2 shows the spectra of the multiple lines reported here with exception of the CO( $J = 3 - 2$ ). Additionally, we present synthetic LTE models for the spectra using XCLASS program (Comito et al. 2005). The data were fitted well with the synthetic model using rotational temperatures, column densities, and sizes of 250 K,  $2 \times 10^{16}$  cm<sup>2</sup>, and 1'', respectively, for the lines SO(8<sub>9</sub>-7<sub>8</sub>), SO<sub>2</sub>(19<sub>1,19</sub>-18<sub>0,18</sub>), HC<sub>3</sub>N(38-37) ( $\nu_t=0$ ), and C<sub>2</sub>H<sub>5</sub>OH(37<sub>8,29</sub>-36<sub>9,28</sub>) and 800 K,  $5 \times 10^{18}$  cm<sup>2</sup>, and 0.5'' for transitions with high excitation temperatures in the lower energy states, HCOCH<sub>2</sub>OH(68<sub>19,49</sub>-67<sub>20,48</sub>) and HCOCH<sub>2</sub>OH(62<sub>13,49</sub>-62<sub>12,50</sub>). This modeling serves as for avoiding the line confusion, and suggest that hot gas is only found in the innermost parts of the hot core. See Table 1 for the rest frequencies and the physical parameters of the lines. The physical parameters of all lines were obtained fitting a Gaussian to the line profile.

In order to be more confident about the detection of the glycol-aldehyde ( $\text{HCOCH}_2\text{OH}$ ) toward W51 North, we have fitted simultaneously many other lines that fall in our 2 GHz bands with our synthetic LTE model using the same parameters as above. We obtained a reasonable agreement between the synthetic model and the detected lines. A full astrochemical analysis of these lines (and other species) is beyond the scope of the present paper in which we concentrate on the spatial distributions of the lines presented in Table 1.

The spectra of the  $\text{SO}(8_9-7_8)$  additionally shows self-absorption possibly due to the molecular gas is falling into the central object (Zapata et al. 2008).

The integrated intensity or moment zero maps of the lines associated with the molecular disk are presented in Figure 3. We have divided these lines into three groups showing the transitions with energy levels with moderate (20-160 K), high (300-800 K), and very high (1400-1600 K) energies and presented them in two different panels. From these images, it is easy to see how the the molecular emission is found in layers with the transitions characterized by high excitation temperatures in their lower energy states (up to 1512 K), and/or critical densities, being concentrated closer to the central high-mass protostar W51 North. This phenomenon confirms clearly that the heating in W51 North is internal. Additionally, molecules with transitions characterized by low and moderate excitation temperatures *i.e.*  $\text{SO}(8_9-7_8)$ ,  $\text{SO}_2(19_{1,19}-18_{0,18})$ ,  $\text{HC}_3\text{N}(38-37)$  ( $\nu_t=0$ ), and  $\text{C}_2\text{H}_5\text{OH}(37_{8,29}-36_{9,28})$  show a central cavity of approximately an angular size of  $0.7''$ , see Table 2. These lines trace thus the molecular Keplerian ring (or toroid) around W51 North reported in  $\text{SO}_2$  by Zapata et al. (2009), see Figure 1. The transition of the molecule  $\text{SO}_2$  utilized by these authors has a similar excitation temperature in the lower energy state as those mentioned above. Note the similarity between the angular size of the inner cavity and the size of the compact dusty circumstellar disk reported by Zapata et al. (2009), see Table 2.

The molecular emission from the transition with a high excitation temperature in the lower energy states (*i.e.*  $\text{HCOCH}_2\text{OH}(68_{19,49}-67_{20,48})$ ) is found peaking at the position of the cavity and showing similar angular sizes to this, see Table 2. This molecule is thus more intimately related with the circumstellar compact dusty disk.

The observational parameters of all lines are shown in Table 2. We noted from Table 1 and 2, there is a correlation between the deconvolved sizes of the molecular emission and the excitation temperatures in lower energy states of each molecular specie. The molecular emission from transitions characterized by high excitation temperatures show to be very compact. This correlation could be obviously obtained for lines that are optically thick with  $T_b \sim \eta T_{ex}$ , where the  $T_b$  is the brightness temperature,  $\eta$  is the filling factor, and  $T_{ex}$  is the excitation temperature.

In the left panel of Figure 3 the emission of the lines  $\text{HCOCH}_2\text{OH}(62_{13,49}-62_{12,50})$  and  $\text{HC}_3\text{N}(38-37)$  ( $\nu_t=0$ ) reveals the presence of a possible warm “companion” located to the northeast of the disk. We have marked the position of this putative companion with a yellow triangle. This “companion” is also observed in  $\text{SO}_2$  at the same position, see Figure 3 of Zapata et al. (2009), and is associated with a group of water maser spots (Imai et al. 2002; Eisner et al. 2002). The position of the “companion” was found by fitting a Gaussian to its  $\text{HCOCH}_2\text{OH}(62_{13,49}-62_{12,50})$  emission. However, it still not clear if the “companion” is real protostar

or if this could be the result of the interaction of the outflow with a high density zone of the molecular cloud.

We do not find any clear evidence of outflowing gas activity associated with this possible “companion” (see also Zapata et al. 2009). Although the blueshifted side of the CO( $J = 3 - 2$ ) outflow has not the same position angle as the redshifted one, this seems not be ejected from the companion. We show how the blueshifted side appears to be more likely ejected from W51 North in Figure 1. We drew a line that crosses this side of the outflow and points directly to the dusty compact disk. The SO<sub>2</sub> and SiO emission indeed show how the outflow is deviated to where the CO( $J = 3 - 2$ ) is located (Zapata et al. 2009). However, more observations in some other molecular outflow tracers are thus necessary to firmly discard the existence of a second outflow in W51 North. It is interesting to note that the possible companion is not observed in the hotter molecular gas tracer HCOCH<sub>2</sub>OH(68<sub>19,49</sub>-67<sub>20,48</sub>) suggesting that it may not as warm as the central massive star.

Figures 4 and 5 show the position-velocity diagrams (PV-diagrams) of different molecules which trace distinct scales of the disk. In Figure 3, we have marked the orientation and position of the PV-cuts. In the left panel of Figure 3 we show a white line with a P.A.=30° that corresponds to the PV-cuts shown in Figure 4. On the other hand, the white line with a P.A.=160° in the right panel corresponds to the the PV-cuts shown in Figure 5.

Figure 4 shows the molecular emission from HC<sub>3</sub>N(38-37) and HCOCH<sub>2</sub>OH(68<sub>19,49</sub>-67<sub>20,48</sub>) located in the innermost parts of the disk, while the PV-diagrams of molecules as SO(8<sub>9</sub>-7<sub>8</sub>), and SO<sub>2</sub>(19<sub>1,19</sub>-18<sub>0,18</sub>), which trace the outermost parts, are presented in Figure 5. The PV-diagrams in Figure 4 reveal that the hot molecular gas closer to the massive protostar is Keplerian. In addition, in this figure we have overlaid the PV-diagram of the LTE Keplerian disk modeled in Zapata et al. (2009), but without an inner cavity and a smaller size. Both structures shown a very good correspondence. The SO(8<sub>9</sub>-7<sub>8</sub>) and SO<sub>2</sub>(19<sub>1,19</sub>-18<sub>0,18</sub>) presented in Figure 5 trace much larger structures similar to the ring reported in Zapata et al. (2009). These molecules in addition show clearly two northwest and southeast high velocity extensions excited by the bipolar outflow mapped in CO( $J = 3 - 2$ ) and SiO( $J = 5 - 4$ ). The PV-diagram of the molecule C<sub>2</sub>H<sub>5</sub>OH(37<sub>8,29</sub>-36<sub>9,28</sub>) shows also Keplerian motions, while that obtained from the molecule HCOCH<sub>2</sub>OH(62<sub>13,49</sub>-62<sub>12,50</sub>) shows a more compact structure without a clear morphology, these diagrams are not presented in this study.

Finally, in Figure 6 we show the spectral energy distribution (SED) from the centimeter, millimeter, and submillimeter wavelengths of W51 North with data obtained from Zapata et al. (2009) and Tang et al. (in prep.). The new value at submillimeter wavelengths presented here shows also to be good fitted with the  $\alpha = 2.8$  value (where the flux density goes as  $S_\nu = \nu^\alpha$ ) found by Zapata et al. (2009).

## 4. Discussion

### 4.1. A multilayer infalling and keplerian disk around W51 North: Connecting the molecular ring and dusty compact disk.

The combined millimeter and submillimeter line observations presented here from the ring and compact dusty disk structures reported in Zapata et al. (2009) suggest that we are seeing a single hot multilayer accreting disk around W51 North (Figure 3). This large molecular disk connects both circumstellar structures, the dusty compact disk, observed at 7 and 1 mm, and the molecular ring mapped in SO<sub>2</sub> in a single structure. Some molecules are found in association with the dusty compact disk while some others with the ring.

The molecular emission associated with the multilayer disk reveals that the molecular emission with transitions with a low excitation temperature in the lower energy states delineates the outer disk and shows a cavity, while such transitions with a high excitation temperature in the lower energy state are found only in the innermost parts of the disk and closer to the central massive protostar(s). One would expect to this physical phenomenon happen in disks or cores around high- and low-mass protostar(s) due to the large optical depths and higher temperatures only found close to the young star. Up to date detailed models of the ensuing chemical evolution at these much higher temperatures do not at present exist.

It still is not clear why we do see an inner cavity on the disk in some molecules with transitions characterized by low and moderate excitation temperatures. This cavity maybe is not a real hole on the disk rather this could be due to photo-dissociation or opacity effects of these molecules toward the innermost parts of the disk. However, we do not discard the possibility that the cavity could be real and formed possibly by the tidal effects of the young multiple massive protostars in the middle of the “ring” as in the case of Ori 139-409 located in Orion South where the protostars have lower masses (Zapata et al. 2010). The molecular emission with transitions characterized by high excitation temperatures in the lower energy states may arise from the possible compact circumstellar disks inside of the cavity that with the actual angular resolution are not resolved. The presence of a binary system at the center of W51 North has been suggested by the precession of the molecular outflow at very small scales found by Eisner et al. (2002). This precession phenomenon may also explain the difference between the position angles of the blueshifted and redshifted components of the CO( $J = 3 - 2$ ) outflow (Figure 1).

The accreting disk hypothesis is supported by the detection of the powerful outflow that emanates with an almost perpendicular orientation to the object. The large disk shows to be Keplerian and with a contracting velocity of about a few km s<sup>-1</sup> as revealed by Zapata et al. (2009). The models presented in Figure 4 were obtained using a slightly different P.A. = 30°, inclination angle of  $i=25^\circ$ , a smaller size (3000 AU), and without an inner cavity than in Zapata et al. (2009).

In Zapata et al. (2009) and here, we have modeled a contracting flattened disk in Keplerian rotation with a central hole, using the disk parametrization from Guilloteau, Dutrey & Simon (1999). The contraction is assumed to have the functional form of free-fall (i.e.  $V_{inf} \propto \frac{1}{\sqrt{r}}$ ), with a reference velocity at the reference radius. However, our resolution is insufficient to determine the exact functional form. The model is for

the same molecules and transitions. A better fit than all other trials in our recurrence was found until we obtained similar structures in our model to those imaged (Figure 4). Most of the physical parameters in the model were constrained in the process. The model fits the observations reasonably well.

In particular, the molecules  $\text{HCOCH}_2\text{OH}(62_{13,49}-62_{12,50})$  and  $\text{HC}_3\text{N}(38-37)$  ( $v_t=0$ ) revealed the possible presence of a warm companion located to the northeast of the disk (Figure 2). We suggest that the companion could be a consequence of disk fragmentation due gravitational instabilities because the disk is extremely large, see for a reference of this phenomenon Kratter & Matzner (2006); Krumholz et al. (2009).

#### 4.2. A possible sequence on the evolution of nascent massive stars?

The multilayer disk imaged in this paper reveals a possible link between the Hyper/Ultra-compact HII regions and the hot cores. These observations suggest a possible sequence on the formation of massive stars. We present this simple sequence in Figure 7, and discuss it as follows:

- *Phase I:* In the first phase, a large and massive pseudo-disk is formed together with a bipolar outflow from a large and dense core. The pseudo-disk is surrounded by an infalling envelope with accretion rates on the order of  $10^{-3} M_{\odot} \text{ yr}^{-1}$ . The molecular emission arising from the circumstellar pseudo-disk could be observed as a single structure without a well defined temperature gradient across it. The pseudo-disks observed toward these objects are not classical circumstellar disks associated with low-mass stars which are centrifugally supported, rather these might be contracting pseudo-disks (see for example the large and massive contracting disks associated with the high-mass protostars AFGL490 and NGC 7538S: Nakamura et al. 1991; Sandell & Wright 2010). The pseudo-disk could be also likely circumbinary or circum-multiple because of the large multiplicity presented on the massive stars.
- *Phase II:* The large and massive pseudo-disk formed earlier is observed now in molecular shells or layers. This object is still surrounded by an infalling envelope. A clear temperature gradient is observed across the disk. The inner cavity could be formed by photodissociation due to the high temperatures close to massive stars or maybe to opacity effects. In this phase, no free-free emission from a HCHII region is detected probably because the infalling molecular gas partially quenches its formation or maybe because the massive central protostar(s) are/is in an early phase with not high enough temperatures to ionize their/its surroundings. W51 North is found here. Another possibility is that maybe there is cluster of late B-type in middle able of forming a strong multilayer molecular disk, but not for developing HCHII regions.
- *Phase III:* A HCHII region appears in the middle of the large multilayer pseudo-disk. At this stage the central massive protostar has the sufficient high temperatures ( $> 10^4 \text{ K}$ ) to ionize its surroundings, see for example the cases of NGC7538 IRS1 (Franco-Hernández & Rodríguez 2004; Sandell et al. 2009) and MWC349 (Tafuya et al. 2004). These sources are maybe variable on time because of the strong accretion from the large disk continues toward the massive central star, see also G24.78+0.08

A1 (Galván-Madrid et al. 2008). There are some sources that might be situated at this phase, see for example, the molecular rotating toroids observed around the UCHII regions G24.78+0.08 A1 and G5.89-0.39 (Su et al. 2009; Beltrán et al. 2006). Moreover, Klaassen et al. (2009) found in a group of HCHII and UCHII regions rotating molecular structures surrounding them. Therefore, the molecular toroids or rings around an UCHII are likely the same structures as in Phase II, but just hotter. The holes observed in these toroids might be due to the photodissociation of some molecules, or maybe to the formation of cavities by the presence of a multiple system of massive stars as mentioned before. In this phase the massive young star(s) might be still accreting ionized material as proposed and described by Keto & Wood (2006).

- *Phase IV:* In this phase the HCHII region expands and ionizes the remnant molecular disk or toroid, and creates an extended H II region surrounding one or maybe multiple young massive stars. The sequence from UCHII to extended HII regions has been discussed by García-Segura & Franco (2004); Franco et al. (2007). If the central star(s) is/are still accreting material, probably ionized material, an outflow show also be present even at this stage.

## 5. Summary

We have observed the massive and young protostar W51 North with the SMA using a high angular resolution and sensitivity at millimeter and submillimeter wavelengths. We give a summary of the results as follows:

- We report the presence of a large and single molecular disk around the object W51 north, and confirm the existence of a single powerful outflow emanating from the disk;
- The molecular emission from the large disk is observed in layers with transitions characterized by high excitation temperatures in the lower states (up to 1512 K) being concentrated closer to the central massive protostar. The molecular emission at low or moderate excitation temperatures additionally exhibits a central cavity with an angular size around  $0.7''$ . This multilayer disk connects the molecular ring and dusty compact disk reported recently toward this object (Zapata et al. 2009). The LTE modeling presented in this study also confirms that the hot gas is only found in the innermost disk.
- A detail study of the kinematics of the molecular gas together with a model of a circumstellar disk in Local Thermodynamic Equilibrium shows that the disk is Keplerian, and is accreting fresh gas to the protostar possibly quenching the formation of a HCHII region;
- The thermal emission of the HCOCH<sub>2</sub>OH reveals the possible presence of a warm companion located to the northeast of the disk, perhaps produced by disk fragmentation or maybe is the interaction of the outflow a high density zone. The molecular emission of the SO and SO<sub>2</sub> is observed in the circumstellar disk as well as in the outflow;

- We modeled all lines with a LTE synthetic spectra. For an assumed source size of 0.5 - 1 arcsec, our modeling yields a column density of  $2 - 6 \times 10^{16-18} \text{ cm}^{-2}$ , a temperature of 250 - 800 K, and a linewidth of  $\sim 5 - 10 \text{ km s}^{-1}$ .

We thank the anonymous referee for many valuable suggestions. This research has made extensive use of the SIMBAD database, operated at CDS, Strasbourg, France, and NASA's Astrophysics Data System. This research made use of the myXCLASS program (<https://www.astro.uni-koeln.de/projects/schilke/XCLASS>), which accesses the CDMS (<http://www.cdms.de>) and JPL (<http://spec.jpl.nasa.gov>) molecular data bases.

## REFERENCES

- Barbosa, C. L., Blum, R. D., Conti, P. S., Damineli, A., & Figuerêdo, E. 2008, *ApJ*, 678, L55
- Beltrán, M. T., Cesaroni, R., Codella, C., et al. 2006, *Nature*, 443, 427
- Cesaroni, R. 2005, in *IAU Symposium*, Vol. 227, *Massive Star Birth: A Crossroads of Astrophysics*, ed. R. Cesaroni, M. Felli, E. Churchwell, & M. Walmsley, 59–69
- Cesaroni, R., Hofner, P., Araya, E., & Kurtz, S. 2010, *A&A*, 509, A50+
- Cesaroni, R., Neri, R., Olmi, L., et al. 2005, *A&A*, 434, 1039
- Comito, C., Schilke, P., Phillips, T. G., et al. 2005, *ApJS*, 156, 127
- Eisner, J. A., Greenhill, L. J., Herrnstein, J. R., Moran, J. M., & Menten, K. M. 2002, *ApJ*, 569, 334
- Franco, J., García-Segura, G., Kurtz, S. E., & Arthur, S. J. 2007, *ApJ*, 660, 1296
- Franco-Hernández, R. & Rodríguez, L. F. 2004, *ApJ*, 604, L105
- Galván-Madrid, R., Rodríguez, L. F., Ho, P. T. P., & Keto, E. 2008, *ApJ*, 674, L33
- García-Segura, G. & Franco, J. 2004, in *Revista Mexicana de Astronomía y Astrofísica Conference Series*, Vol. 22, *Revista Mexicana de Astronomía y Astrofísica Conference Series*, ed. G. Garcia-Segura, G. Tenorio-Tagle, J. Franco, & H. W. Yorke, 131–135
- Gaume, R. A., Johnston, K. J., & Wilson, T. L. 1993, *ApJ*, 417, 645
- Ho, P. T. P., Moran, J. M., & Lo, K. Y. 2004, *ApJ*, 616, L1
- Imai, H., Watanabe, T., Omodaka, T., et al. 2002, *PASJ*, 54, 741
- Keto, E. & Wood, K. 2006, *ApJ*, 637, 850
- Klaassen, P. D., Wilson, C. D., Keto, E. R., & Zhang, Q. 2009, *ApJ*, 703, 1308

- Kratter, K. M. & Matzner, C. D. 2006, *MNRAS*, 373, 1563
- Krumholz, M. R., Klein, R. I., McKee, C. F., Offner, S. S. R., & Cunningham, A. J. 2009, *Science*, 323, 754
- Kurtz, S. 2005, in *IAU Symposium*, Vol. 227, *Massive Star Birth: A Crossroads of Astrophysics*, ed. R. Cesaroni, M. Felli, E. Churchwell, & M. Walmsley, 111–119
- Kurtz, S., Cesaroni, R., Churchwell, E., Hofner, P., & Walmsley, C. M. 2000, *Protostars and Planets IV*, 299
- Leurini, S., Hieret, C., Thorwirth, S., et al. 2008, *A&A*, 485, 167
- Lizano, S. 2008, in *Astronomical Society of the Pacific Conference Series*, Vol. 387, *Massive Star Formation: Observations Confront Theory*, ed. H. Beuther, H. Linz, & T. Henning, 232–+
- Mehring, D. M. 1994, *ApJS*, 91, 713
- Nakamura, A., Kawabe, R., Ishiguro, M., et al. 1991, *ApJ*, 383, L81
- Osorio, M., Lizano, S., & D’Alessio, P. 1999, *ApJ*, 525, 808
- Rolfs, R., Schilke, P., Zhang, Q., et al. 2009, in *Astronomical Society of the Pacific Conference Series*, Vol. 417, *Astronomical Society of the Pacific Conference Series*, ed. D. C. Lis, J. E. Vaillancourt, P. F. Goldsmith, T. A. Bell, N. Z. Scoville, & J. Zmuidzinas, 215–+
- Sandell, G., Goss, W. M., Wright, M., & Corder, S. 2009, *ApJ*, 699, L31
- Sandell, G. & Wright, M. 2010, *ArXiv e-prints*
- Schneps, M. H., Moran, J. M., Genzel, R., et al. 1981, *ApJ*, 249, 124
- Schreyer, K., Henning, T., van der Tak, F. F. S., Boonman, A. M. S., & van Dishoeck, E. F. 2002, *A&A*, 394, 561
- Scoville, N. Z., Carlstrom, J. E., Chandler, C. J., et al. 1993, *PASP*, 105, 1482
- Sewilo, M., Churchwell, E., Kurtz, S., Goss, W. M., & Hofner, P. 2004, *ApJ*, 605, 285
- Su, Y., Liu, S., Wang, K., Chen, Y., & Chen, H. 2009, *ApJ*, 704, L5
- Tafuya, D., Gómez, Y., & Rodríguez, L. F. 2004, *ApJ*, 610, 827
- van der Tak, F. F. S. 2004, in *IAU Symposium*, Vol. 221, *Star Formation at High Angular Resolution*, ed. M. G. Burton, R. Jayawardhana, & T. L. Bourke, 59–+
- Walmsley, M. 1995, in *Revista Mexicana de Astronomia y Astrofisica Conference Series*, Vol. 1, *Revista Mexicana de Astronomia y Astrofisica Conference Series*, ed. S. Lizano & J. M. Torrelles, 137–+
- Xu, Y., Reid, M. J., Menten, K. M., et al. 2009, *ApJ*, 693, 413

- Zapata, L. A., Ho, P. T. P., Schilke, P., et al. 2009, *ApJ*, 698, 1422
- Zapata, L. A., Palau, A., Ho, P. T. P., et al. 2008, *A&A*, 479, L25
- Zapata, L. A., Schilke, P., & Ho, P. T. P. 2010, *MNRAS*, 402, 2221
- Zhang, Q., Ho, P. T. P., & Ohashi, N. 1998, *ApJ*, 494, 636

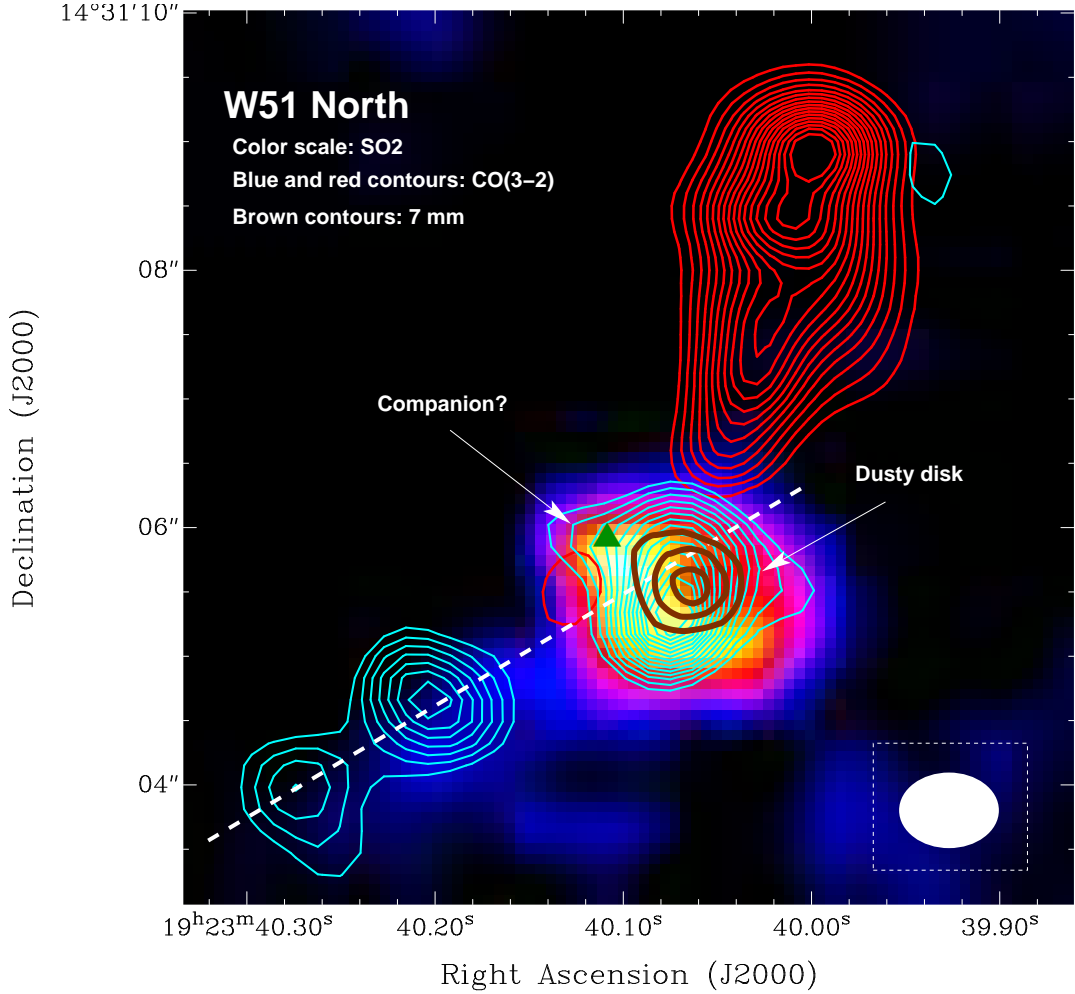


**Fig. 1.**— Overlay of the SO<sub>2</sub>(22<sub>2,20</sub>-22<sub>1,21</sub>) moment zero emission (color image), the 7 mm continuum emission from the compact dusty disk (brown contours), and the CO( $J = 3 - 2$ ) moment zero emission from the bipolar outflow (blue and red contours). The SO<sub>2</sub> and the 7 mm images were taken from Zapata et al. (2009). The integrated velocity range for the CO( $J = 3 - 2$ ) is from +20 to +50 km s<sup>-1</sup> for the blueshifted gas, and from +70 to +120 km s<sup>-1</sup> for the redshifted gas. The brown contours are the 10%, 13%, and 16% of the peak of the 7 mm continuum emission, the peak is 100 mJy beam<sup>-1</sup>. The synthesized beam of the CO( $J = 3 - 2$ ) contour image is 0.71'' × 0.57'' with a P.A. of 87.6° and is shown in the bottom right corner. The green triangle marks the position of the possible companion reported in this paper. The white dashed line shows how the blueshifted side of the outflow seems to be more likely energized from the central massive protostar W51 North rather than the possible companion.

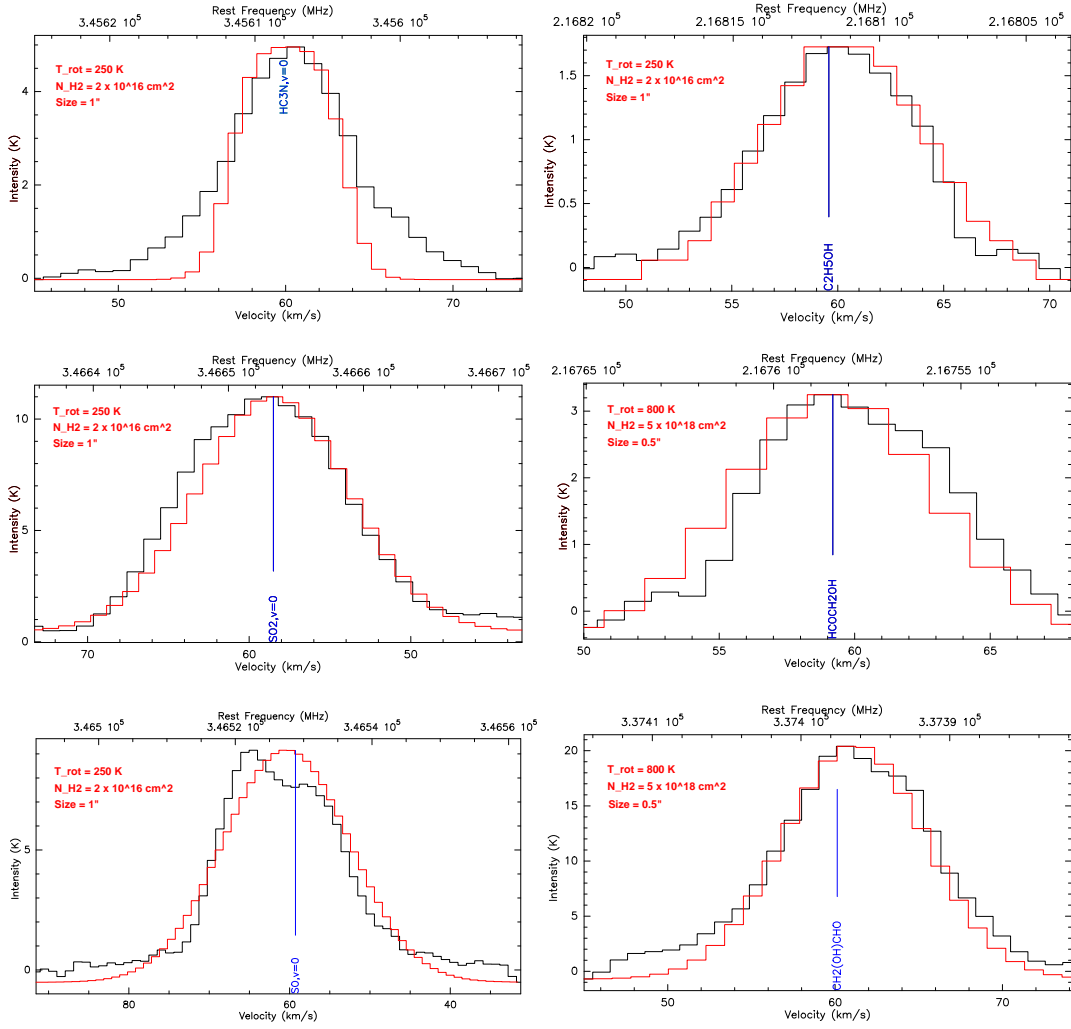
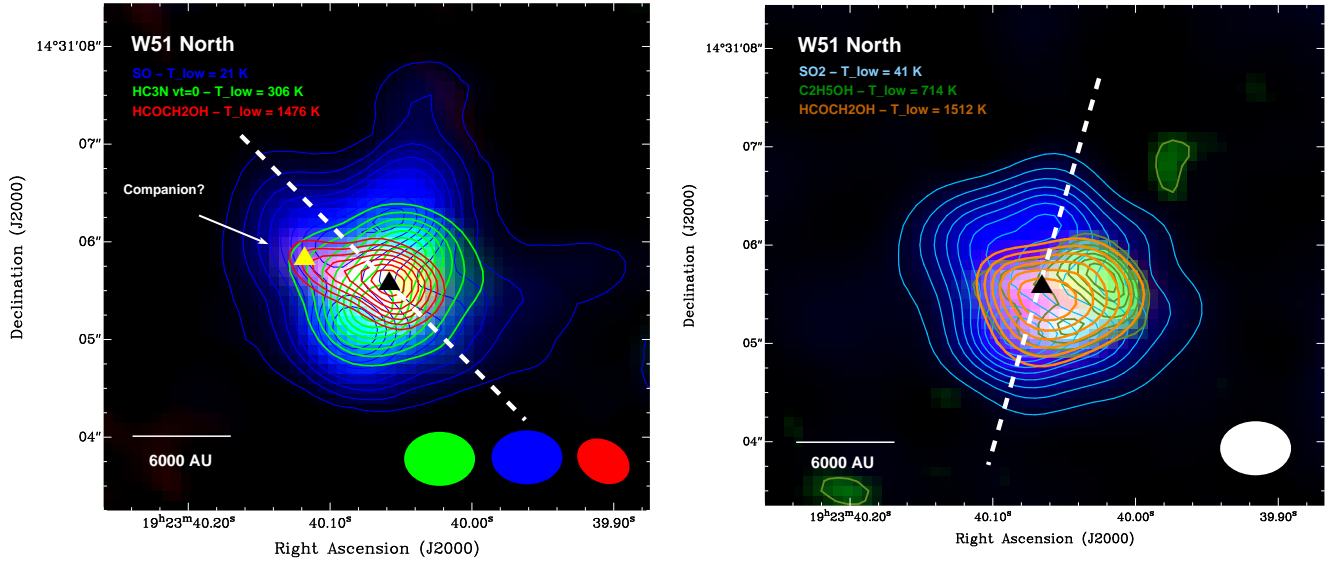


Fig. 2.— Spectra from the selected millimeter and submillimeter lines observed toward W51 North. The red line represents in all panels the synthetic spectrum obtained for the best fitting solution with the parameters shown in each panel. The spectra was obtained from the average of the total emission in each line using the task “inspect” of MIRIAD.



**Fig. 3.**— Composite images of the molecular emission from the circumstellar large disk around the massive protostar W51 North. Left: The blue color scale and the contours are representing the integrated emission of the SO( $8_9-7_8$ ), green ones the HC<sub>3</sub>N( $38-37$ ) ( $\nu_l=0$ ), and the red ones the HCOCH<sub>2</sub>OH( $62_{13,49}-62_{12,50}$ ). The blue contours are from 5% to 90% with steps of 10% of the peak of the line emission, the peak is  $53 \text{ Jy beam}^{-1} \text{ km s}^{-1}$ . The green contours are from 30% to 90% with steps of 10% of the peak of the line emission, the peak is  $26 \text{ Jy beam}^{-1} \text{ km s}^{-1}$ . The red contours are from 30% to 90% with steps of 10% of the peak of the line emission, the peak is  $3.5 \text{ Jy beam}^{-1} \text{ km s}^{-1}$ . The synthesized beams of the millimeter and submillimeter observations are shown on the right bottom corner. Right: The light blue color scale and the contours are representing the integrated emission of the SO<sub>2</sub>( $19_{1,19}-18_{0,18}$ ), green ones the C<sub>2</sub>H<sub>5</sub>OH( $37_{8,29}-36_{9,28}$ ), and the orange ones the HCOCH<sub>2</sub>OH( $68_{19,49}-67_{20,48}$ ). The light blue contours are from 30% to 90% with steps of 10% of the peak of the line emission, the peak is  $38 \text{ Jy beam}^{-1} \text{ km s}^{-1}$ . The green contours are from 30% to 90% with steps of 10% of the peak of the line emission, the peak is  $2 \text{ Jy beam}^{-1} \text{ km s}^{-1}$ . The orange contours are from 30% to 90% with steps of 10% of the peak of the line emission, the peak is  $27 \text{ Jy beam}^{-1} \text{ km s}^{-1}$ . The synthesized beam of the three measurements is the same and is shown on the right bottom corner. The triangles represent the position of the two possible embedded massive protostars as suggested by the hot molecular emission of the HCOCH<sub>2</sub>OH( $62_{13,49}-62_{12,50}$ ) and HC<sub>3</sub>N( $38-37$ ) ( $\nu_l=0$ ). The white dashed line in both panels represents the position and orientation where the PV-diagrams shown in Figures 4 and 5 were computed.

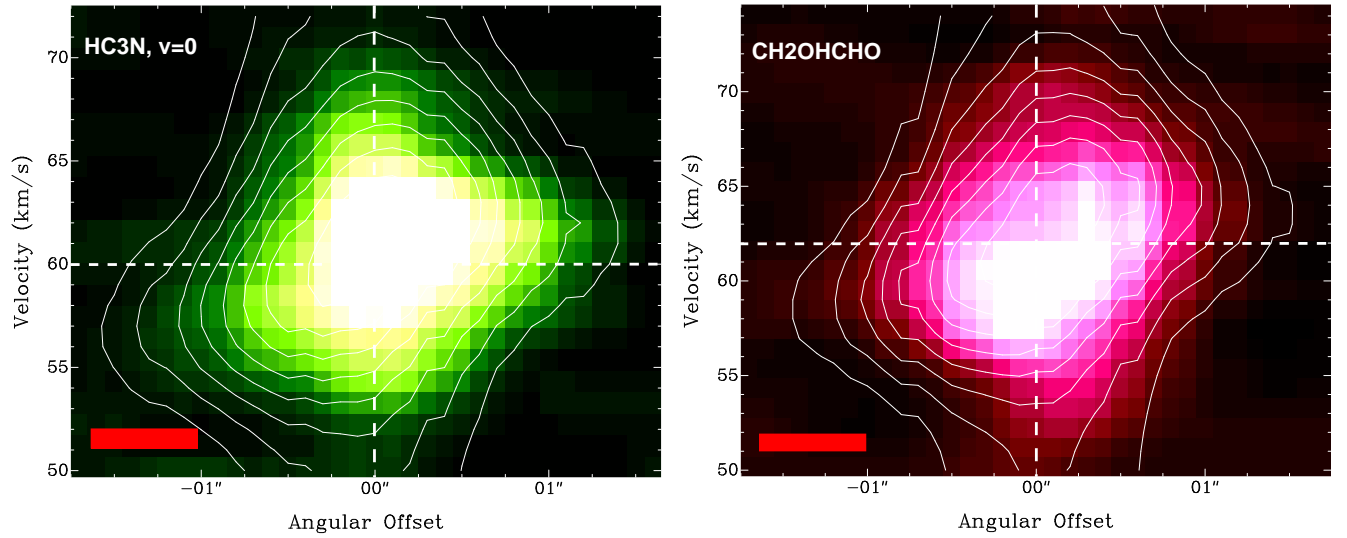


Fig. 4.— Position-velocity diagrams of the  $\text{HC}_3\text{N}(38-37)$  (green scale color), and the  $\text{HCOCH}_2\text{OH}(68_{19,49}-67_{20,48})$  (pink scale color) line emission from the circumstellar disk. The PV diagrams were computed at a P.A. =  $30^\circ$  (see Figure 3). These diagrams are additionally overlaid with the position-velocity diagram at same P.A. of our Keplerian disk model (contours). The contours are from 20% to 90% with steps of 10% of the peak of the line emission of our model. The units of the horizontal axis are in arcseconds. The systemic LSR radial velocity of the ambient molecular cloud is about  $60 \text{ km s}^{-1}$ , see Table 1. The angular and spectral resolutions are shown in each panel on the bottom left corner. The synthesized beam of both images is  $0.71'' \times 0.57''$  with a P.A. of  $87.6^\circ$ . The spectral resolution was smoothed to  $1 \text{ km s}^{-1}$ . The origin in the horizontal axis is at R.A. =  $19\text{h}23\text{m}40.05\text{s}$ , decl. =  $14^\circ 31' 05.0''$  (J2000.0).

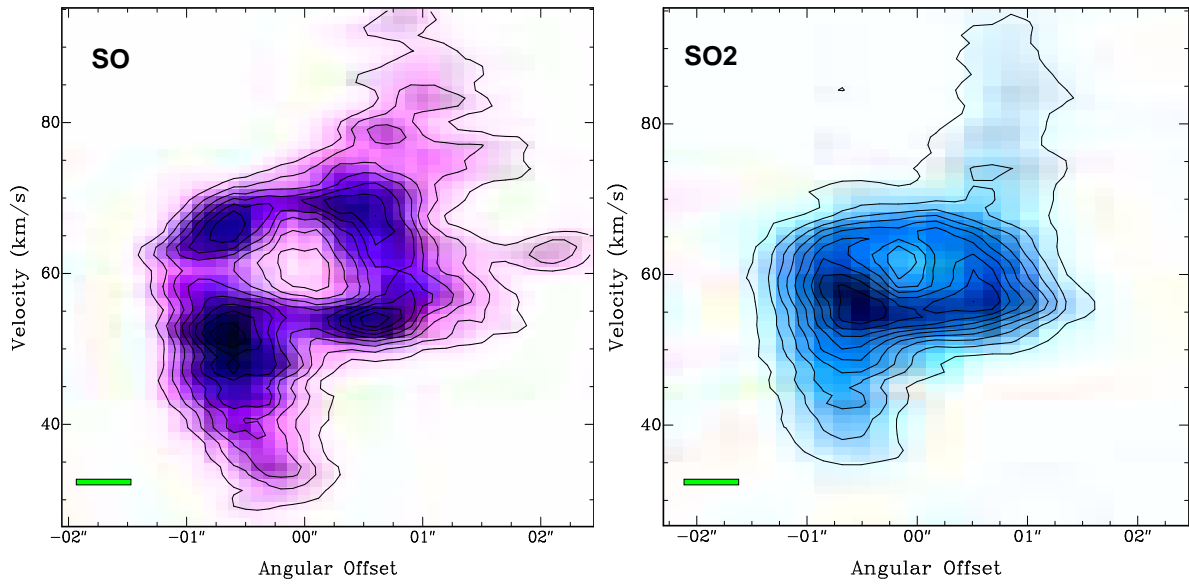


Fig. 5.— Position-velocity diagrams for the  $\text{SO}(8_9-7_8)$  and the  $\text{SO}_2(19_{1,19}-18_{0,18})$  from the large circumstellar disk and the outflow. They were computed at a P.A. of  $160^\circ$  (see Figure 3). The contours in both panels are from 10% to 90% with steps of 10% of the peak of the line emission. The units of the horizontal axis are in arcseconds. The systemic LSR radial velocity of the ambient molecular cloud is about  $60 \text{ km s}^{-1}$ , see Table 1. The angular and spectral resolutions are shown in each panel on the bottom left corner. The synthesized beam of both images is  $0.71'' \times 0.57''$  with a P.A. of  $87.6^\circ$ . The spectral resolution was smoothed to  $1 \text{ km s}^{-1}$ . The origin in the horizontal axis is at R.A. =  $19\text{h}23\text{m}40.05\text{s}$ , decl. =  $14^\circ 31' 05.0''$  (J2000.0).

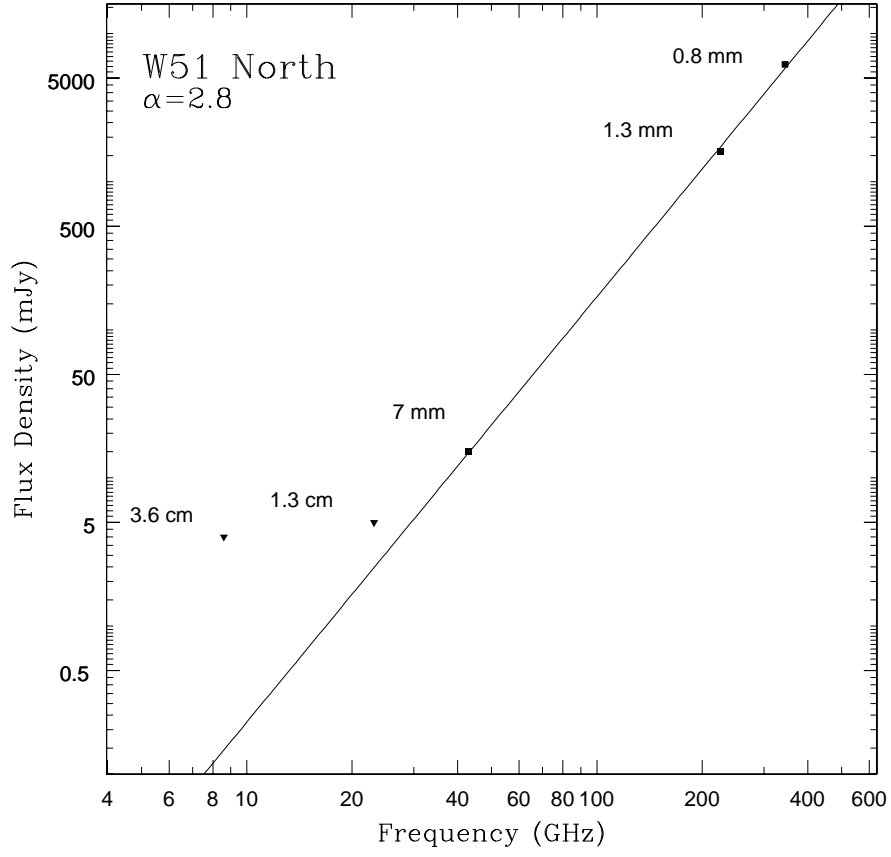


Fig. 6.— SED for the source W51 North combining 3.6 cm, 1.3 cm, 7 mm, 1.3 mm and 0.8 mm continuum data. The millimeter data were obtained from Zapata et al. (2009) and the submillimeter data was obtained from Tang et al. (in prep.). The respective error bars were smaller than the squares and are not presented here. The line is a least-squares power-law fit (of the form  $S_\nu \propto \nu^\alpha$ ) to the spectrum. Note that the value of  $\alpha=2.8$  obtained by Zapata et al. (2009) fit very well all millimeter and submillimeter measurements. The 1.3 cm point is a upper limit ( $5\sigma=5$  mJy) obtained from Figure 1 of Eisner et al. (2002). The 3.6 cm point is a upper limit ( $5\sigma=4$  mJy) obtained from Figure 5 of Mehringer (1994).

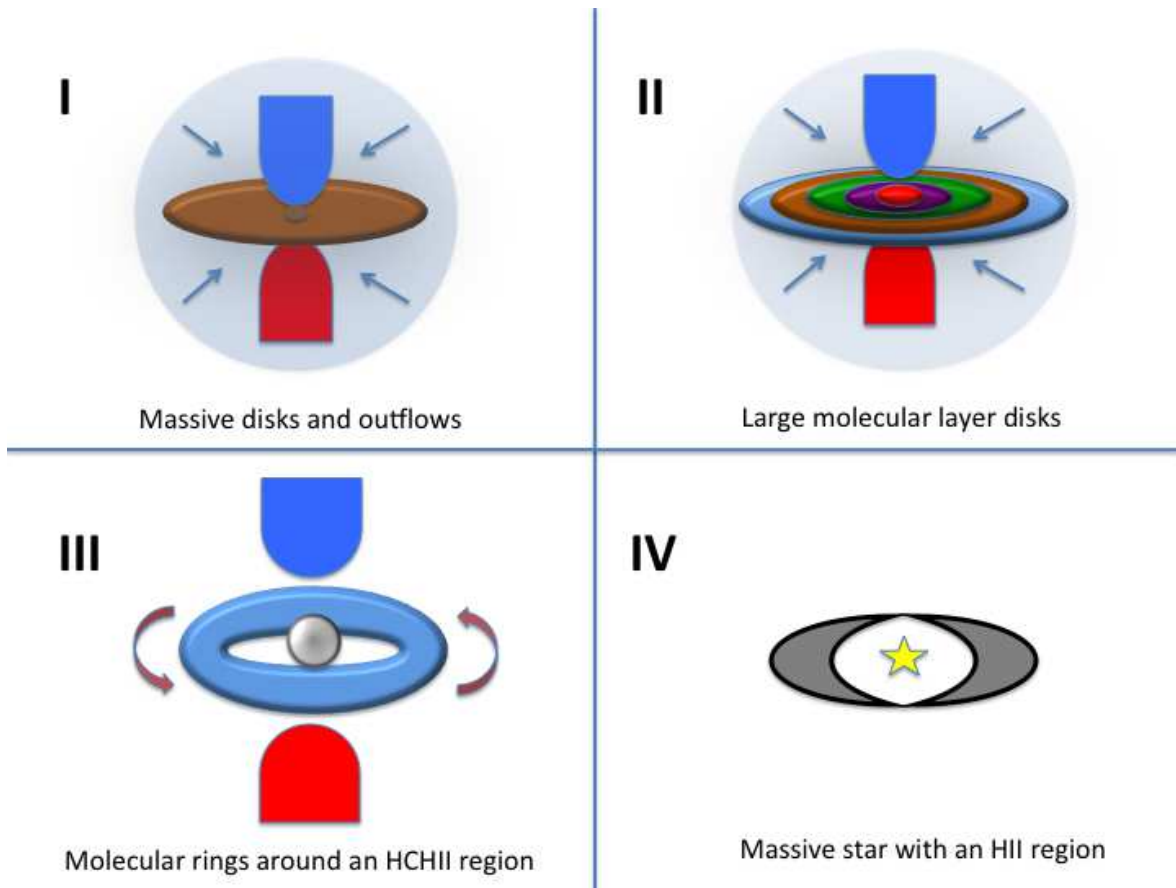


Fig. 7.— A very simple diagram showing the different evolutionary phases of a massive protostar. In this diagram, we do not included multiplicity for simplicity.